

# A comparative assessment of hysteresis and dead beat controllers for performances of three phase shunt active power filtering

Rakhee Panigrahi, Bidyadhar Subudhi\*, Prafulla Chandra Panda

*Department of Electrical Engineering, National Institute of Technology  
Rourkela, 769008, India*

## Abstract

This paper presents the performance evaluation of two control techniques, namely Dead Beat Control (DBC) and Hysteresis Band Control (HBC), in a three phase Shunt Active Power Filter (SAPF). The choice and implementation of the current controllers is vital for the achievement of a satisfactory filtering performance. Although these techniques have been applied previously to design SAPF for single phase distorted power system signals, in this paper we extend them to three phase distorted power system signals. In order to test the effectiveness of these two controllers, extensive simulations were conducted using MATLAB/simulink. The results obtained show the superiority of the hysteresis current controller over the dead beat controller in terms of exhibiting fast transient response and computational simplicity. These results are valid with real-time Opal-RT results.

**Keywords:** Power quality, Shunt active power filter, Voltage source inverter, Hysteresis band control, Dead beat control, Pulse width modulation, Kalman filter

## 1. Introduction

Extensive usage of power electronic devices such as diodes, thyristor rectifiers, lighting equipments, uninterruptible power supplies (UPS) etc. introduces increased harmonics into the power system. Harmonic currents and voltages also yield increased  $I^2R$  losses, over voltage, saturation of transformer core and a reduced lifespan of sensitive equipment. Therefore, suitable harmonics estimation and filtering need to be employed so that good power quality can be assured.

The areas of interest in harmonic studies include modeling, measurements, mitigation and estimation of fundamental as well as harmonic components. Accurate analysis of power system measurements is essential to determine harmonic levels.

Use of grid-connected power electronic converters to improve power quality in power distribution systems is one of the best solutions for achieving improved performance and stability for the elimination of harmonic distortion, power factor correction, balancing loads, and voltage regulation. An active power filter (APF) is a suitable choice for filtering the harmonics. It has two configurations: the shunt active power filter which is placed in parallel with the load; the other being a series active power filter that is employed for voltage correction and is connected in line with the load. It may be noted that the performance

\*Corresponding author

*Email addresses:* rpanigrahi99@gmail.com (Rakhee Panigrahi), bidyadharnitrkl@gmail.com (Bidyadhar Subudhi\*), pcpanda1948@gmail.com (Prafulla Chandra Panda)

of an APF depends heavily on the inverter characteristics, the control method used, and the accuracy of the reference signal generator.

The methods for extracting harmonic references from measured load currents are classified into two types of compensation techniques [1–4] namely time domain and the frequency domain. In the time domain, the more commonly applied methods are the instantaneous reactive power theory (PQ-theory) and the synchronous reference frame transformation (SRF-method). Their dynamic performances deteriorate when the line voltages are distorted. On the other hand frequency domain methods can be used in both single phase and three phase systems, as well as in online and offline APFs. These methods are generally based on the discrete Fourier Transform (DFT), which allows direct extraction of each one of the harmonic components of the load current and simplifies the cancellation in selective mode. However, the main disadvantage of this method is poor response to distorted line voltage.

Kalman filtering has been used as the reference current estimator, in which the Kalman gains are calculated to minimize the square of the expected errors between the actual values and the estimated system states. Hence, the tracking of time varying harmonics becomes easier. It provides the instantaneous values of each one of the harmonic components of the load current, simplifying the retrieval of the reference signal for compensation in a global manner and it is insensitive to distortion in line voltage.

Once the current references have been determined, the APF must have the capability to accurately track such references even in the presence of sudden slope variations. Among the reported current control techniques [5–12], hysteresis current control and dead beat control have the most effective performance in controlling APFs. Hysteresis control directly compares the measured and reference currents and selects a switching state accordingly. It has the fastest speed of response, not being delayed by any A/D conversion process or calculation time. Among digital solutions, the dead beat algorithm is known to ensure the best dynamic response. It can operate with constant APF switching frequency and is easy to implement using simple processors. However, no comparative assessment has been performed for the above two

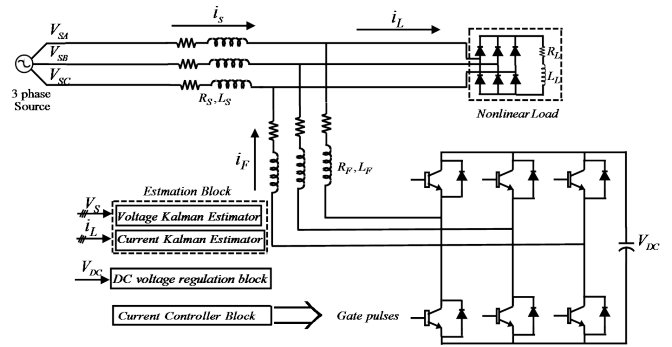


Figure 1: Structure of Shunt Active Power Filter

controllers which applied to three phase distorted power systems. To this end, the aforementioned control techniques such as HBC and DBC were employed for the active filtering of a three phase power system and their performances are presented with discussions.

The paper is organised as follows. Section 2 describes the development and modeling of a three phase SAPF. Section 3 presents the control strategy of the active power filter. Section 4 shows the implementation of current control techniques. A comparative assessment of HBC and DBC are illustrated and discussed in section 5, followed by a conclusion.

## 2. Development of a three phase shunt active power filter

The functional diagram of a SAPF based on a voltage source inverter for compensation of the current harmonics generated by a nonlinear load is shown in Fig. 1. The control structure of the active filter composed of three basic blocks, namely: Estimation block, DC voltage regulation block and Current controller block. Two Kalman estimators are used, one for the estimation of load current and another for the source voltage. The voltage regulation of the dc bus is performed by adjusting the small amount of real power flowing into the capacitor, thus compensating the losses in the active power filter. The current controller block decides the switching pattern of the active power filter according to the error signal generated by the actual and reference signal.

### 2.1. Non-linear Load Modeling

A three-phase diode bridge rectifier with R-L load is considered as a nonlinear load. Due to the presence of source inductance, six overlapping and six non-overlapping conduction intervals occur in a cycle [13]. During a non-overlapping interval, only two devices will conduct, while during an overlapping interval three devices of the bridge will conduct simultaneously. The dynamic equations during non-overlap and overlap intervals are given in (1) and (2), respectively

$$p i_d = \frac{(V_0 - (2R_S + R_L) i_d - 2V_d)}{2L_S + L_L} \quad (1)$$

$$p i_d = \frac{(V_0 - (1.5R_S + R_L) i_d - 2V_d)}{1.5L_S + L_L} \quad (2)$$

where  $R_S$ ,  $L_S$  are the elements of source impedance,  $V_d$  is the drop across diode pairs,  $R_L$  and  $L_L$  are the elements of load impedance,  $i_d$  is the load current flowing through the diode pairs and 'p' is the differential operator ( $d/dt$ ).  $V_0$  is the AC side line voltage segments during overlap intervals and non-overlap intervals based on diode pair conduction.

### 2.2. DC Capacitor Voltage Regulation

In steady state, the real power supplied by the source should be equal to the real power demand of the load plus a small power to compensate the losses in the active filter. Thus, DC capacitor voltage can be maintained at a reference value. However, when the load condition changes, the real power balance between the mains and the load will be disturbed. The real power difference is to be compensated by the DC capacitor. This changes the DC capacitor voltage,  $V_{DC}$ , away from the reference voltage,  $V_{DCref}$ . In order to maintain satisfactory operation of the active filter, the peak value of the reference current must be adjusted to proportionally change the real power drawn from the source. This real power charged/discharged by the capacitor compensates the real power consumed by the load. If DC capacitor voltage is recovered and attains the reference voltage, the real power supplied by the source is supposed to be equal to that consumed by the load again.

P-I (proportional-integral) controller is used to regulate the dc capacitor voltage of the APF. The dc

bus capacitor voltage  $V_{DC}(n)$  is sensed with set reference voltage  $V_{DCref}(n)$ . The resulting voltage error  $V_e(n)$  at  $n$ th sample instant is expressed as:

$$V_e(n) = V_{DCref}(n) - V_{DC}(n) \quad (3)$$

The output of the PI voltage controller is,

$$V_0(n) = V_0(n-1) + K_p(V_e(n) - V_e(n-1)) + K_i V_e(n) \quad (4)$$

where  $K_p$  and  $K_i$  are the proportional and integral gain constants of the voltage regulator.  $V_0(n-1)$  and  $V_e(n-1)$  are output of the controller and voltage error at  $(n-1)$  th sampling instant. This output  $V_0(n)$  of the voltage controller is limited to safe permissible values and the resulting output is taken as the peak of supply current  $I_{max}$ .

### 2.3. Digital Kalman filter for estimation of voltage and current

This paper employs the Kalman Filter for estimation of the load current and the source voltage waveforms of the distorted power system. The Kalman filter [14–18] is a state observer which optimally estimates the states of a system when the system is corrupted by noise and observations are taken as noisy. Kalman Filtering provides optimal estimation of the system state variables in real-time with respect to the minimization of the mean square error and adjusts the value of the estimation during each sampling interval. Recursive Kalman filtering is adaptable in that it adjusts dynamically to the system's evolution, allowing signal tracking in real time. The predictive Kalman filtering loop is obtained by advancing the estimated value of the state variables in one step.

#### 2.3.1. Recursive Kalman filtering Loop

A first order autoregressive model with process noise and measurement noise can be expressed by,

$$x(n) = \phi x(n-1) + w(n-1) \quad (5)$$

$$z(n) = Hx(n) + v(n) \quad (6)$$

Equation (5) and (6) are the signal and measurement model respectively.  $x(n)$  is the time varying state variable at instant  $n$ ,  $\phi$  is the state transition matrix,

$w(n)$  is the process noise vector,  $z(n)$  is the measurement of the signal,  $H$  is the observation matrix,  $v(n)$  is the vector of white noise with zero mean and variance  $\sigma_v^2$  and the estimated state is given by

$$\hat{x}(n) = \phi \hat{x}(n-1) + K(n) [z(n) - H\phi \hat{x}(n-1)] \quad (7)$$

where  $K(n)$  is the Kalman gain which is updated using the following expression

$$K(n) = P(n | n-1) H^T [HP(n | n-1) H^T + R(n)]^{-1} \quad (8)$$

where  $R(n)$  is the measurement noise covariance at the instant  $n$ .  $P(n | n-1)$  is the value of the covariance estimated with the error at instant  $n$  calculated with the value of the real covariance obtained at instant  $n-1$ ,

$$P(n | n-1) = \phi P(n-1 | n-1) \phi^T + Q(n-1) \quad (9)$$

where  $Q(n-1)$  is the process noise covariance and defines the covariance of  $w(n-1)$ .  $P(n-1 | n-1)$  is the real value of the covariance of the error at instant  $n-1$ . Then the real value of the covariance of the error at instant  $n$  is expressed by

$$P(n | n) = P(n | n-1) - K(n) HP(n | n-1) \quad (10)$$

### 2.3.2. Predictive Kalman filtering Loop

In this case, the digital filter is based on:

$$\hat{x}(n+1 | n) = \phi \hat{x}(n | n-1) + G(n) \quad (11)$$

where  $G(n)$  can be expressed as

$$G(n) = K(n) [z(n) - H\hat{x}(n | n-1)] \quad (12)$$

and

$$K(n) = \phi P(n | n-1) H^T [HP(n | n-1) H^T + R(n)]^{-1} \quad (13)$$

The covariance estimated with the error at instant  $n+1$  calculated with the value of the real covariance at instant  $n$  is

$$P(n+1 | n) = [\phi - K(n)H] P(n | n-1) \phi^T + Q(n) \quad (14)$$

### 3. System Signal Model

Voltage and current signals in power systems can be described using state equations which take into account the frequency components in-phase and in-quadrature [13]. Since each frequency component requires two state variables, the total number of state variables is  $2m$ . The fixed reference axes must be considered, where the estimation value corresponds to the instantaneous values of the input signal.

If  $x_{mp}$  and  $x_{mq}$  are in-phase and in-quadrature components of the  $m$ th harmonic of a distorted signal. The state equation description of the  $m$ th harmonic of a distorted signal in fixed reference axes with angular frequency  $m\omega$  can be expressed as

$$x_m(k) = \begin{bmatrix} x_{1p}(k) \\ x_{1q}(k) \\ \vdots \\ x_{mp}(k) \\ x_{mq}(k) \end{bmatrix} \quad (15)$$

$$H_m = \begin{bmatrix} 1 & 0 & \dots & 1 & 0 \end{bmatrix} \quad (16)$$

$$\phi = \begin{bmatrix} \phi_1 & 0 & \dots & 0 \\ 0 & \ddots & & \vdots \\ \vdots & & \ddots & 0 \\ 0 & \dots & 0 & \phi_m \end{bmatrix} \quad (17)$$

$$\phi_m = \begin{bmatrix} \cos(m\omega\Delta t) & -\sin(m\omega\Delta t) \\ \sin(m\omega\Delta t) & \cos(m\omega\Delta t) \end{bmatrix} \quad (18)$$

### 4. Dead Beat Current Control

The objective of the dead-beat current control [19–21] of shunt active power filter is to manipulate the power circuit so that the actual current generated by active power filter  $i_F$  follows the reference current  $i_F^*$  as closely as possible. Fig. 2 shows the single arm of APF which can be used to derive the dead beat controller, where  $R_F$  is considered to be negligible due to the very small value.

Applying Kirchhoff's voltage law in Fig. 2 leads to the following equation

$$V_a(t) - V_s(t) = L_F \frac{di_F(t)}{dt} \quad (19)$$

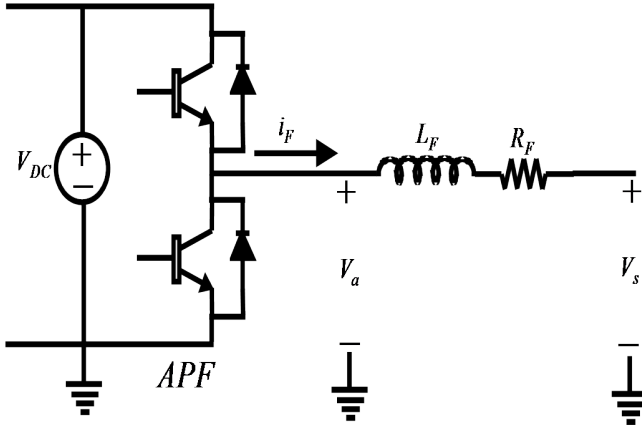


Figure 2: Single phase arm of APF to derive dead beat controller

where  $V_a$  and  $V_s$  are the inverter output voltage and source voltage respectively.  $L_F$  and  $i_F$  are the filter inductance and filter current respectively. The discrete time system equations, developed in the alpha beta fixed reference frame, have the following expression:

$$i_F(n+1) = \frac{T_{SW}}{L_F} [V_a(n) - V_s(n)] + i_F(n) \quad (20)$$

where  $T_{SW}$  is the switching period and the inverter voltage at  $n+1$  instant with modelled inductance  $L_{Fm}$  is given by,

$$V_a(n-1) = \frac{L_{Fm}}{T_{SW}} [i_F^*(n) - i_F(n)] + 2V_s(n) - V_a(n) \quad (21)$$

where line voltage  $V_s$  is either measured or estimated. The line voltage estimation can be obtained using the algorithm:

$$e_s(n-1) = V_a(n-1) + \frac{L_{Fm}}{T_{SW}} [i_F(n-1) - i_F(n)] \quad (22)$$

where  $e_s$  stands for estimation of  $V_s$  and then substituting  $V_s(n)$  with  $e_s(n-1)$  in Eq. (21).

#### 4.1. SAPF Control unit using DBC

Fig. 3 shows the control block diagram of SAPF using dead beat control. The Voltage Kalman Filter (VKF) and Current Kalman Filter (CKF) are applied

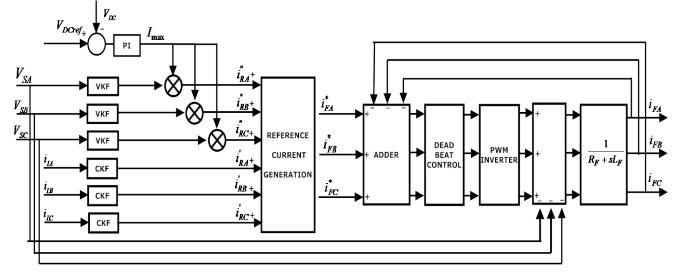


Figure 3: SAPF Control Unit Design Using DBC

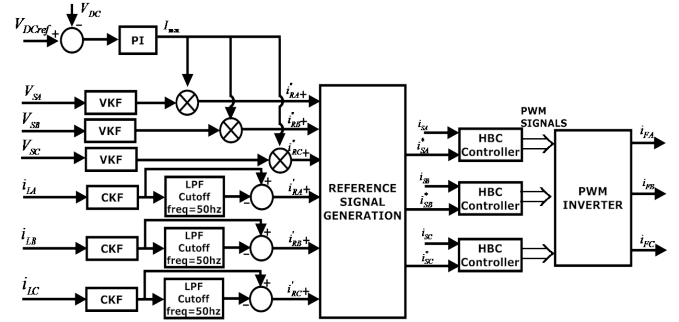


Figure 4: Proposed SAPF Control Unit Design Using HBC

to the line voltage and the load current respectively. The current estimator is a 20 states discrete Kalman filter, corresponding to the first 10 odd current harmonics ( $3^{rd}$ ,  $5^{th}$ ,  $7^{th}$ ...  $21^{st}$ ) and it gives instantaneous values of in-phase and in-quadrature components of load current harmonics,  $i'_{RA}$ . The voltage estimator is a 10 states discrete Kalman filter, corresponding to the first 5 odd voltage harmonics and it gives the instantaneous values of the in-phase fundamental component with per-unit magnitude. This component is modulated by output  $I_{max}$  of a PI controller, which is applied to the dc voltage  $V_{DC}$  with  $V_{DCref}$  as reference value and the modulated signal is  $i''_{RA}$ . The term  $i'_{RA}$  corresponds to load current disturbances and the term  $i''_{RA}$  corresponds to the active current component at fundamental frequency derived from supply voltage.

These frequency components are added to obtain the reference current,  $i_{FA}^*$  for phase A only. The similar case holds for the other two phases. The computational lag associated with digital signal processing is avoided with the use of the predictive Kalman Filtering loop. The filter current  $i_{FA}$  is obtained as a voltage difference on the link inductor ( $L_F$ ,  $R_F$ ) and this voltage is composed of the inverter output voltage and the source voltage. The current controller has to

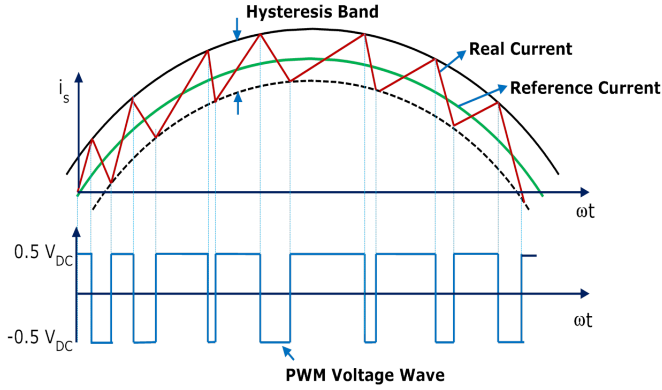


Figure 5: Principle of Hysteresis Controller

ensure that both reference current and filter current are injected into the PCC.

## 5. Hysteresis Current Control

Fig. 5 illustrates the basic concept of the hysteresis control scheme. The controller generates the sinusoidal reference current of desired magnitude and frequency that is compared with the actual line current. If the current exceeds the upper limit of the hysteresis band, the upper switch of the inverter arm is turned off and the lower switch is turned on. As a result, the current starts to decay. If the current crosses the lower limit of the hysteresis band, the lower switch of the inverter arm is turned off and the upper switch is turned on. As a result, the current gets back into the hysteresis band [22, 23]. Hence, the actual current is forced to track the reference current within the hysteresis band.

### 5.1. SAPF Control unit using HBC

The SAPF control block diagram with HBC technique is shown in Fig. 4. In this case, a low pass Butterworth filter ( $2^{nd}$  order) of cutoff frequency 50 Hz combining with Kalman filter (CKF) is used to generate the reference current components,  $i'_{RA}$ ,  $i'_{RB}$ ,  $i'_{RC}$ . Here the VKF plays the same role as in the DBC case. The addition of  $i'_{RA}$  and  $i''_{RA}$  gives the reference  $i^*_{SA}$ . Similarly, reference currents  $i^*_{SB}$ ,  $i^*_{SC}$  are generated for phases  $B$  and  $C$  respectively. The actual currents ( $i_{SA}$ ,  $i_{SB}$ ,  $i_{SC}$ ) and reference currents ( $i^*_{SA}$ ,  $i^*_{SB}$ ,  $i^*_{SC}$ ) are compared within the hysteresis band in three controllers separately and the current controller

Table 1: Simulation parameters

$V_s$ , V	100	$F$ , Hz	50
$R_S$ , $\Omega$	1	$L_S$ , mH	0.55
$R_L$ , $\Omega$	6.7	$L_L$ , mH	0.02
$R_F$ , $\Omega$	1	$L_F$ , mH	2.7
$V_{DC}$ , V	170	$V_{DCref}$ , V	250
$K_p$	0.015	$K_i$	6.99
$C_{DC}$ , $\mu F$	2000	$f_{sw}$ , kHz	10

decides the switching pattern of the devices in APF. The switching logic is formulated as follows:

if  $i_{SA} < (i^*_{SA} - hb)$ , upper switch is OFF and lower switch is ON in leg 'A' of the APF;

if  $i_{SA} > (i^*_{SA} + hb)$ , upper switch is ON and lower switch is OFF in leg 'A' of the APF.

Similarly, the switches in legs 'B' and 'C' are activated. Here, 'hb' is the width of the hysteresis band.

The three phase voltages  $V_{FA}$ ,  $V_{FB}$ ,  $V_{FC}$  are generated on the input side of the inverter in terms of dc capacitor voltage  $V_{DC}$  and on/off status of the devices of each leg  $T_A$ ,  $T_B$  and  $T_C$  as

$$V_{FA} = \frac{V_{DC}}{3} (2T_A - T_B - T_C) \quad (23)$$

$$V_{FB} = \frac{V_{DC}}{3} (-T_A + 2T_B - T_C) \quad (24)$$

$$V_{FC} = \frac{V_{DC}}{3} (-T_A - T_B + 2T_C) \quad (25)$$

The filter currents ( $i_{FA}$ ,  $i_{FB}$ ,  $i_{FC}$ ) can be calculated using the following differential equations such as,

$$p i_{FA} = \frac{1}{L_F} R_F i_{FA} + V_{SA} - V_{FA} \quad (26)$$

$$p i_{FB} = \frac{1}{L_F} R_F i_{FB} + V_{SB} - V_{FB} \quad (27)$$

$$p i_{FC} = \frac{1}{L_F} R_F i_{FC} + V_{SC} - V_{FC} \quad (28)$$

## 6. Simulation Result

The SAPF model using the DBC and HBC methods as shown in Fig. 3 and Fig. 4 were simulated using MATLAB/simulink. The parameters used for the simulation are shown in Table 1, where  $V_s$  is the

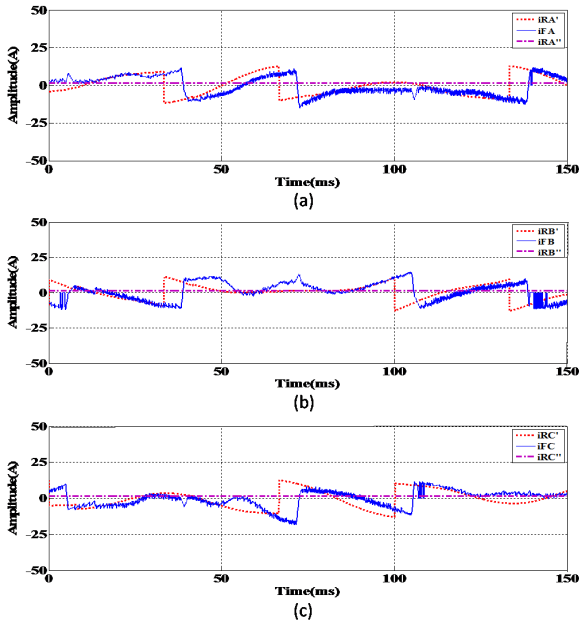


Figure 6: Estimated Currents and Compensating Current for (a) Phase-A, (b) Phase-B, (c) Phase-C using DBC method

supply voltage,  $F$  is the supply frequency,  $K_p$  and  $K_i$  are PI-controller constants, and  $f_{sw}$  is the power converter switching frequency. The switching frequency was taken as 10 kHz. The distortions of voltages applied to nonlinear load composed of three phase diode bridge rectifier with RL load as shown in Fig. 1 are taken as 5.03%. The results obtained by using the DBC and HBC methods are presented below.

Fig. 6 shows the estimation results of reference compensating currents along with the actual compensating current using the DBC method for three phases. The compensating currents track the reference currents, which are clearly shown in Fig. 6. The predictive effect of the Kalman filter estimation method compensates the computational lags. The source currents after compensation are given in Fig. 7 and it can be shown that they are nearly sinusoidal and in same phase with the source voltage, even if under distorted source voltage conditions.

Fig. 11 shows the reference currents generated using the HBC method for three phases and Fig. 8 shows the compensating waveforms, which are equal and opposite to load current harmonics such that harmonics should be cancelled perfectly.

As seen from Fig. 9, the compensated source currents are proportional to the measured voltages. Despite

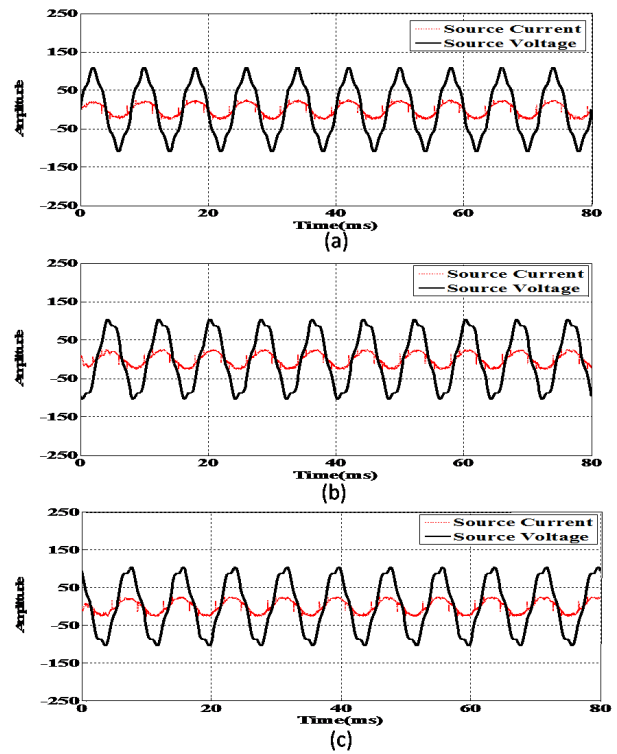


Figure 7: Source Voltage and Source Current before and after compensation for a) Phase-A, (b) Phase-B, (c) Phase-C using DBC method

Table 2: THD% calculation for source current for phase-A

Meth-ods	Source Current Before Compensation, %	Source Current After Compensation, %
DBC	30.3	5.83
HBC	30.3	5.56

the distortion in source voltage, the calculation accuracy of current compensation is not affected. The source current spectra before and after compensation are shown in Fig. 10 using the DBC and HBC methods respectively. The harmonics amplitudes are smaller in the HBC method when compared with the DBC method for phase-A.

Table 2 shows the THD% calculation of source current for phase-A using both the DBC and the HBC method. In both cases the source current has harmonic distortion of 30.3% before compensation. But after compensation, it is about 5.83% for the DBC method and 5.56% for the HBC method. The distort-

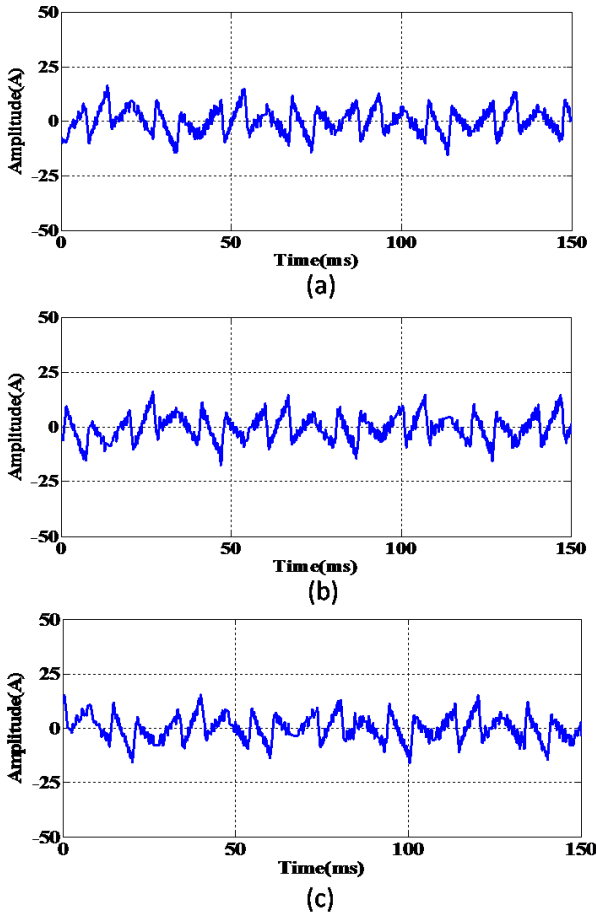


Figure 8: Compensating Current Waveforms for, (a) Phase-A, (b) Phase-B, (c) Phase-C using HBC method

tion is greater in the DBC method than in the HBC method.

### 7. Validation with Real-time Opal-RT Result

To further evaluate the performance of the proposed active filter, a real-time simulation model for the same system described earlier is also implemented and its experimental setup is displayed in Fig. 12. The modeling is based on Opal-RT [23], which is a fully digital electromagnetic transient power system simulator that operates in real time. Because the solution is in real time, the simulator can be connected directly to a hardware controller or other devices. Thus, real-time simulation provides a convenient medium for network-level power system analysis and equipment testing. Fig. 13 and 14 show the waveforms from the Opal-RT real-time simulator. As can be seen, these compare well to the detailed sim-

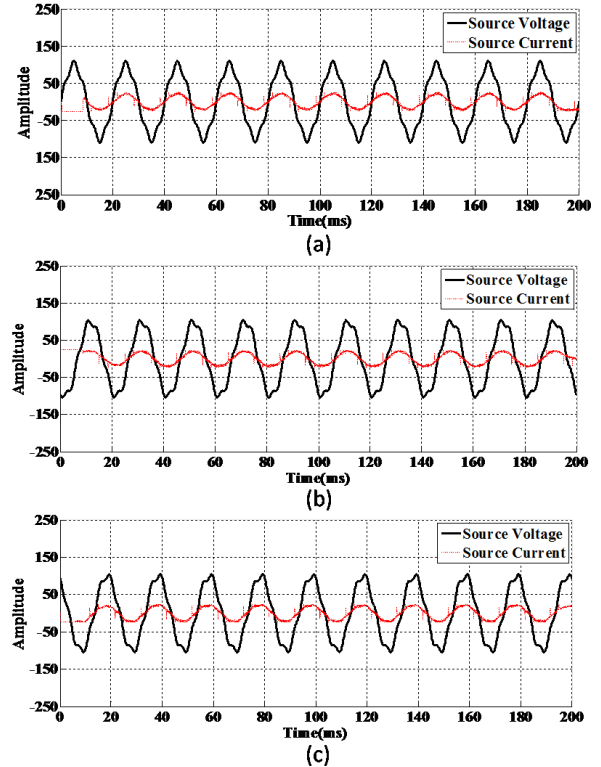


Figure 9: Source Voltage and Source Current before and after compensation for a) Phase-A, (b) Phase-B, (c) Phase-C using HBC method

ulation results.

### 8. Conclusions

This paper compares the dynamic performance of the two popular current control techniques, i.e., Dead Beat Control and Hysteresis Current Control in Shunt Active Power filter connected parallel to the non-linear load. The current control techniques are tested in both simulation and real-time Opal-RT Lab to shape the source current to be as sinusoidal as possible while feeding harmonic rich current to the nonlinear diode rectifier load. Irrespective of fixed switching frequency, the DBC method is incapable of achieving a satisfactory performance level. The results of the comparison show a certain superiority of the Hysteresis Current Control. Indeed, the performance of this control strategy is excellent for the performance indices considered in the paper, i.e., harmonic content, THD and the line current spectra under distorted source voltage conditions ( $\approx 5.03\%$ ). Here the Kalman filter has been developed for cor-

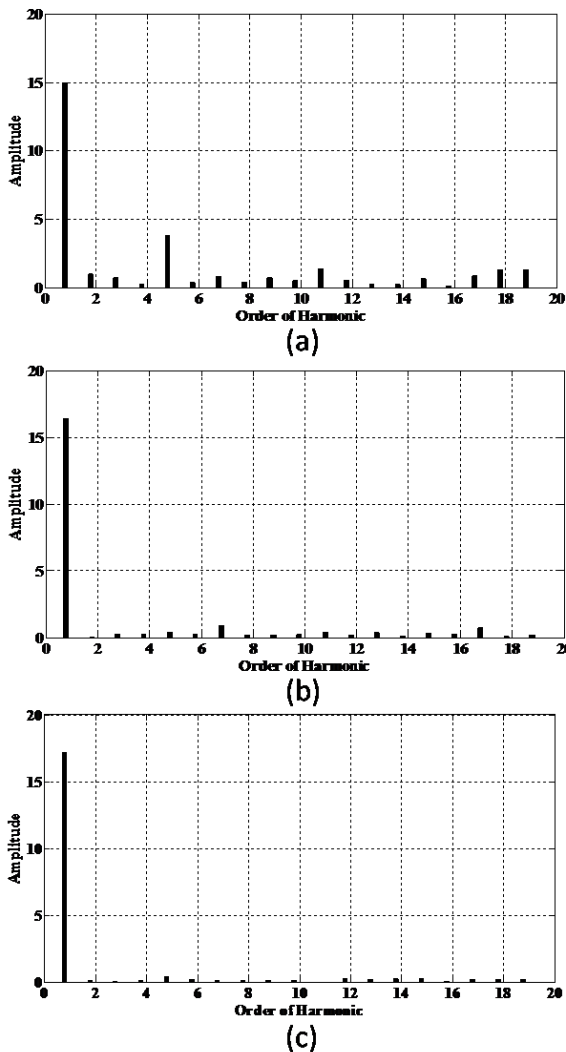


Figure 10: (a) Source Current spectrum before compensation for phase-A, (b) Source Current spectrum after compensation with DBC, (c) Source Current spectrum after compensation with HB

rect estimation of reference current and cancellation of harmonics globally.

### Acknowledgments

This work was supported by the Central Power Research Institute of Bangalore (vide no. 3/5/R & D/RSOP/2011).

### References

[1] S. J. Huang, J. C. Wu, D. D. Divan, A control algorithm for three phase three-wired active power filters under non-ideal voltages, *IEEE Transactions on Power Electronics* 14 (1999) 753–760.

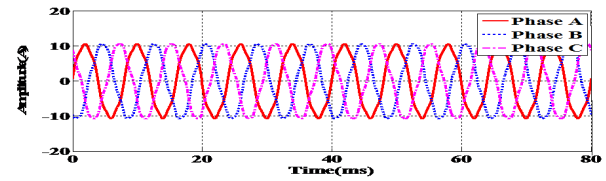


Figure 11: Reference currents generated for a) Phase-A, (b) Phase-B, (c) Phase-C using HBC method



Figure 12: Typical Experimental Setup

- [2] X. Yuan, W. Merk, H. Stemmler, J. Allmeling, Stationary-frame generalized integrators for current control of active power filters with zero steady-state error for current harmonics of concern under unbalanced and distorted operating conditions, *IEEE Transactions on Industry Applications* 38 (2002) 523–532.
- [3] V. Soares, P. Verdelho, G. D. Marques, An instantaneous active and reactive current component method for active filters, *IEEE Transactions on Power Electronics* 15 (2000) 660–669.
- [4] P. Mattavelli, A closed-loop selective harmonic compensation for active filters, *IEEE Transactions on Industry Applications* 37 (2001) 81–89.
- [5] M. P. Kazmierkowski, M. A. Dzieniakowski, Review of current regulation techniques for three-phase pwm inverters, in: *Proc. IEEE IECON'94, 1994*, pp. 567–575.
- [6] M. A. Rahman, T. S. Radwan, A. M. Osheiba, A. E. Lashine, Analysis of current controllers for voltage-source inverter, *IEEE Transactions on Industrial Electronics* 44 (4) (1997) 477–485.
- [7] L. Malesani, P. Tenti, A novel hysteresis control method for current controlled vsi pwm inverters with constant modulation frequency, *IEEE Transactions on Industry Applications* 26 (1990) 88–92.
- [8] S. Buso, L. Malesani, P. Mattavelli, Comparison of current control techniques for active filter applications, *IEEE Transactions on Power Electronics* 45 (1998) 722–729.
- [9] T. Kawabata, T. Miyashita, Y. Yamamoto, Dead beat control of three phase pwm inverter, *IEEE Transactions on Power Electronics* 5 (1990) 21–28.
- [10] Y. Xiaojie, L. Yongdong, A shunt active power filter using dead-beat current control, in: *IEEE 2002 28th Annual Conference-IECON 02, Vol. 1, Industrial Electronics So-*

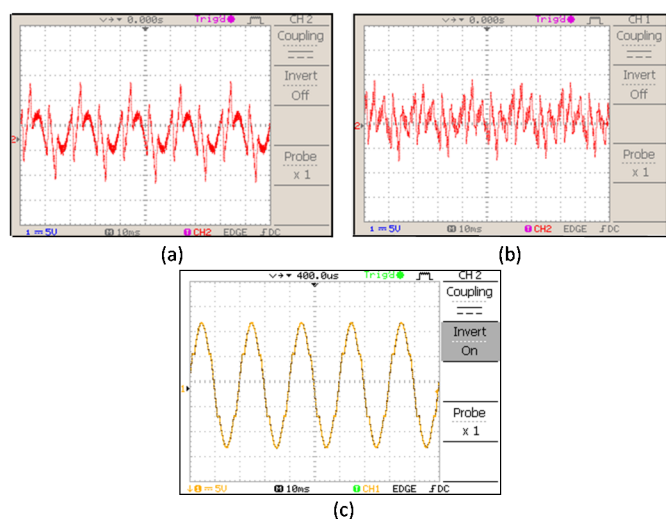


Figure 13: Opal-RT result for phase-A: (a) Compensating current with DBC, (b) Compensating current with HBC, (c) Line voltage

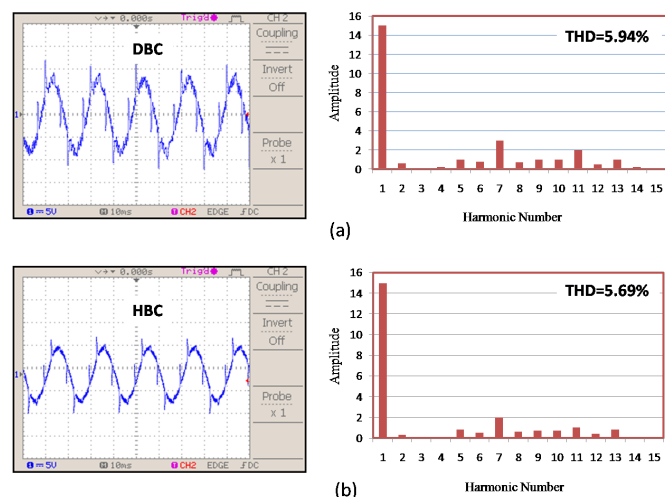


Figure 14: Opal-RT result for phase-A: (a) Source current with its spectrum in DBC, (b) Source current with its spectrum in HBC

- ciety, 2002, pp. 633–637.
- [11] A. Kawamura, T. Haneyoshi, R. G. Hoft, Deadbeat controlled pwm inverter with parameter estimation using only voltage sensor, in: *Conf. Rec. IEEE PESC'86*, 1986, pp. 576–583.
- [12] L. Malesani, P. Tenti, E. Gaio, R. Piovan, Improved current control technique of vsi pwm inverters with constant modulation frequency and extended voltage range, *IEEE Transactions on Industry Applications* 27 (1991) 365–369.
- [13] A. A. Girgis, W. B. Chang, E. B. Makram, A digital recursive measurements scheme for on-line tracking of power system harmonics, *IEEE Transactions on Power Delivery* 6 (3) (1991) 1153–1160.
- [14] V. Moreno, A. Pigazo, R. I. Diego, Reference estimation technique for active power filters using a digital kalman algorithm, in: *Proc. IEEE 10th International Conf. on Harmonics and Quality of Power (ICHQP'02)*, Rio de Janeiro, Brazil, 2002.
- [15] V. M. Moreno, A. P. Lopez, R. I. D. Gracias, Reference current estimation under distorted line voltage for control of shunt active power filters, *IEEE Transactions on Power Electronics* 19 (4) (2004) 988–994.
- [16] Z. G. Zhang, S. C. Chan, A recursive frequency estimator using linear prediction and a kalman-filter-based iterative algorithm, *IEEE Transactions on Circuits and Systems* 55 (6) (2008) 576–580.
- [17] M. S. Sachdev, H. C. Wood, N. G. Johnson, Kalman filtering applied to power system measurements for relaying, *IEEE Transactions on Power Apparatus and Systems* PAS-104 (12) (1985) 3565–3573.
- [18] R. A. Zadeh, A. Ghosh, G. Ledwich, Combination of kalman filter and least-error square techniques in power system, *IEEE Transactions on Power Delivery* 25 (4) (2010) 2868–2880.
- [19] Y. Xiaojie, L. Yongdong, A shunt active power filter using dead-beat current control, *industrial electronics society*, in: *IEEE 2002 28th Annual Conference-IECON 02*, Vol. 1, 2002, pp. 633–637.
- [20] H. Abu-Rub, J. Guzinski, Z. Krzeminski, H. A. Toliyat, Predictive current control of voltage-source inverters, *IEEE Transactions on Industrial Electronics* 51 (3) (2004) 585–593.
- [21] L. Malesani, P. Mattavelli, S. Buso, Robust dead-beat current control for pwm rectifiers and active filters, *IEEE Transactions on Industry Applications* 35 (3) (1999) 613–620.
- [22] C.-T. Pan, T.-Y. Chang, An improved hysteresis current controller for reducing switching frequency, *IEEE Transactions on Power Electronics* 9 (1) (1994) 97–104.
- [23] RT-Lab Professional.  
URL <http://www.opal-rt.com/product/rt-lab-professional>
- [24] M. Areds, J. Hafner, K. Heumann, Three-phase four-wire shunt active filter control strategies, *IEEE Transactions on Power Electronics* 12 (1997) 311–318.
- [25] P. T. Cheng, S. Bhattacharya, D. D. Divan, Line harmonics reduction in high-power systems using square-wave inverters-based dominant harmonic active filter, *IEEE Transactions on Power Electronics* 14 (1999) 265–272.
- [26] M. El-Habrouk, M. K. Darwish, P. Mehta, Active power filters: A review, in: *Proc. Inst. Elect. Eng.*, Vol. 147, 2000, pp. 403–413.
- [27] B. Singh, K. Al-Haddad, A. Chandra, A review of active filters for power quality improvement, *IEEE Transactions on Industrial Electronics* 46 (1999) 960–971.
- [28] P. Verdelho, G. D. Marques, An active power filter and unbalanced current compensator, *IEEE Transactions on Industrial Electronics* 44 (3) (1997) 321–328.